Considerations on the Mechanical Dynamics of Interconnected Flux Three-Pole Magnetic Bearings

V.R. Vasco [a], A.C.Del Nero Gomes [b], D.F.B. David [c], J.A. Santisteban [c]

[a] Instituto de Pesquisas da Marinha, Rua Ipiru 02, 21931-090, Rio de Janeiro, Brazil
[b] Universidade Federal do Rio de Janeiro, Centro de Tecnologia, Rio de Janeiro, Brazil
[c] Universidade Federal Fluminense, Rua Passo da Pátria 156, 20420-240, Niteroi, Brazil

***Abstract*—This work presents a step-by-step procedure on how to get the reluctance forces in the optimal three-pole magnetic bearing. These forces are analyzed near the equilibrium point, where linearization produces satisfactory results. Besides that, a linear dynamical system is proposed based on the operation under four types of disturbances, shaft with constant angular speed and small displacements over the center.**

I. INTRODUCTION

Active magnetic bearings are devices that allows a shaft to have contactless support in a rotation machine. They can be built in many different sizes and configurations, being the most common the 8-pole configuration. However, as pointed out in [1], the minimum number of poles that allow generation of reluctance forces in two dimensions is three. In comparison with other types, three-pole magnetic bearings are suitable to compact devices, as they have more space between poles allowing better heat dissipation, sensor installation and also less coil winding.

Chen and Hsu proposed in [2] an optimal design for the three-pole active magnetic bearing, optimizing the cupper loss and reducing the number of amplifiers to two. He also found the relation between winding thickness and pole width that give best results.

In [3], Hsu and Chen presented a feedback linearization of the nonlinear voltage-controlled system, changing variables to consider the magnetic fluxes as part of the states. In [4], the same authors study and compare linear and nonlinear control techniques. They simulated the state-space feedback control alone, feedback linearization with state-space feedback and finally feedback linearization with integral sliding mode control.

In [5], Chen et al. validate the control techniques presented in [4] with experimental tests that were made with and without motor in the shaft. Linear and nonlinear techniques were used. In [6], Meeker and Maslen proposed a new model to the reluctance forces with the aim to facilitate to use a three-phase motor drive.

Chen, in [7] proposed a robust voltage-controller via backstepping, with two stages of integral sliding mode control. More recently, Kiani et al proposed in [8] a hybrid control as a nonlinear control option for the three-pole magnetic bearing configuration and Chen, in [9], presented a sensorless smooth control technique, where the displacements of the rotor are estimated by electrical sensors, allowing reduction of costs.

This study comes to show a detailed look at the reluctance forces that appear in the three-pole configuration, as well as the linearization by Taylor expansion series in order to analyze their behavior near the equilibrium point. Using a similar procedure presented in [10] and [11], with the linearized forces information, a linear dynamical system was modelled considering four types of external disturbances on the system.

II. MODELLING OF MAGNETIC CIRCUITS AND MAGNETIC FORCES

In order to obtain the magnetic force equations of the three-pole magnetic bearing, it is necessary to analyze its magnetic circuit. Fig. 1 illustrates the axial view of the magnetic bearing that will be studied and the magnetic flux path that was created due to the current applied in one coil. The area of each pole is A_c, the air gap between the stator and rotor is h and the magnetic constant $\mu_0 = 4\pi.10^{-7}$ H/m.

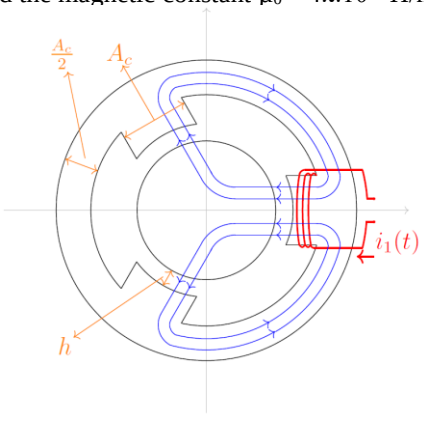

Figure 1. Indication of the magnetic flux path due to application of current in the windings of coil in pole 1.

To analyze the total magnetic flux path created by the windings, it is necessary to analyze them separately and, in the end, add them up to see the result. It is used the right-hand

rule to find the direction of the magnetic field caused by a current in a wire. Naming the poles and coils from 1 to 3 in the counterclockwise direction (beginning from the pole at 0º) and using the notation ϕ_{ik} to indicate the flux that cross the gap in the '*i*' pole due to the current from the coil '*k*', Figures 2, 3 and 4 shows the flux generated by each current. It is important to notice that in this paper the current i_2 is modelled with opposite direction than the currents of the other two coils.

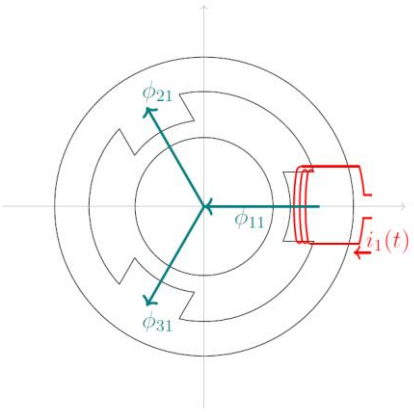

Figure 2. Indication of the magnetic flux path due to application of current in the windings of coil in pole 1.

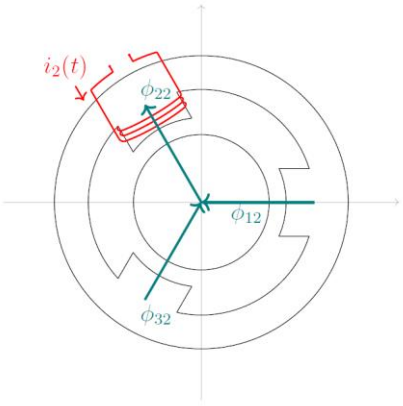

Figure 3. Indication of the magnetic flux path due to application of current in the windings of coil in pole 2.

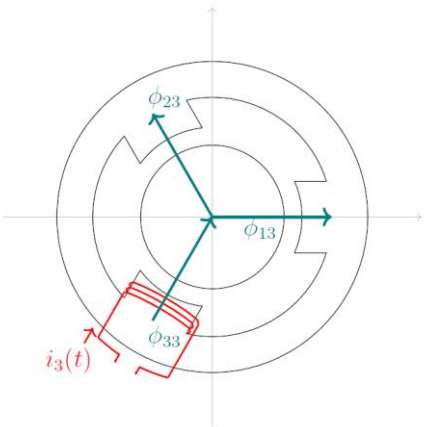

Figure 4. Indication of the magnetic flux path due to application of current in the windings of coil in pole 3.

With notation ϕ_i representing the total flux crossing the pole "*i*", with positive sign pointing to the center of the rotor, as indicated in Figure 5, and considering that the system doesn't suffer any air and ferromagnetic losses, the total magnetic flux in each pole is given by equations (1), (2) and (3).

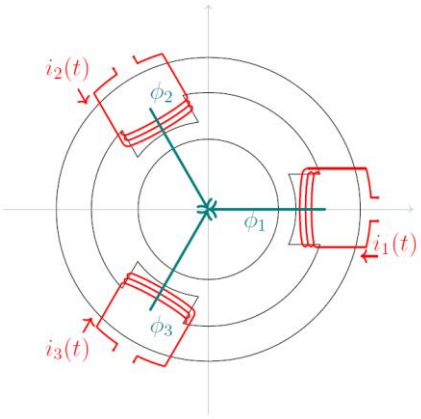

Figure 5. Indication of the total magnetic flux in each pole.

$$\phi_1 = +\phi_{11} + \phi_{12} - \phi_{13} \tag{1}$$

$$\phi_2 = -\phi_{21} - \phi_{22} - \phi_{23} \tag{2}$$

$$\phi_3 = -\phi_{31} + \phi_{32} + \phi_{33} \tag{3}$$

Given that n_c is the number of turns in each coil, i_j and F_j is, respectively, the current and magnetomotive force in the "*j*"th pole, the magnetomotive force is given by equation (4), and the reluctance by equation (5):

$$\mathcal{F}_j = n_c i_j, j = 1, 2, 3 \tag{4}$$

$$\mathcal{R}_i = \frac{h}{\mu_0 A_c}, i = 1, 2, 3 \tag{5}$$

The equivalent magnetic circuit corresponding to the coil 1, is shown in Figure 6.

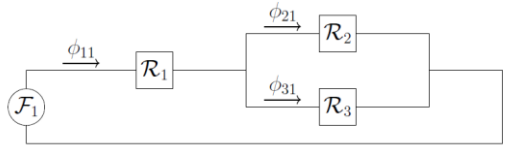

Figure 6. Magnetic Circuit Associated with coil 1.

The expressions obtained is given by equations (5) to (8).

$$\mathcal{F}_1 = n_c i_1 \tag{5}$$

$$\phi_{11} = n_c i_1 \frac{\mathcal{R}_2 + \mathcal{R}_3}{N} \tag{6}$$

$$\phi_{21} = n_c i_1 \frac{\mathcal{R}_3}{N} \tag{7}$$

$$\phi_{31} = n_c i_1 \frac{\mathcal{R}_2}{N} \tag{8}$$

In which the variable *N* is given by the equation (9).

$$N = \mathcal{R}_1\mathcal{R}_2 + \mathcal{R}_1\mathcal{R}_3 + \mathcal{R}_2\mathcal{R}_3 \tag{9}$$

Similarly, as above, the diagram corresponding to coil 2 is shown in Figure 7 and the corresponding expressions in equations (10) to (13).

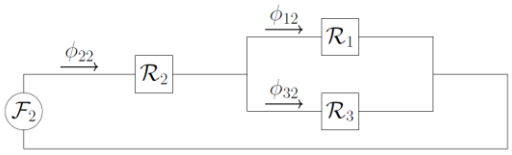

Figure 7. Magnetic Circuit Associated with coil 2.

$$\mathcal{F}_2 = n_c i_2 \tag{10}$$

$$\phi_{12} = n_c i_2 \frac{\mathcal{R}_3}{N} \tag{11}$$

$$\phi_{22} = n_c i_2 \frac{\mathcal{R}_1 + \mathcal{R}_3}{N} \tag{12}$$

$$\phi_{32} = n_c i_2 \frac{\mathcal{R}_1}{N} \tag{13}$$

Finally, for coil 3, the magnetic circuit is given by Figure 7 and the expressions in equations (14) to (17).

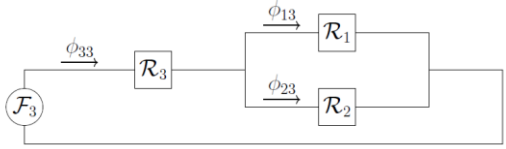

Figure 8. Magnetic Circuit Associated with coil 3.

$$\mathcal{F}_3 = n_c i_3 \tag{14}$$

$$\phi_{13} = n_c i_3 \frac{\mathcal{R}_2}{N} \tag{15}$$

$$\phi_{23} = n_c i_3 \frac{\mathcal{R}_1}{N} \tag{16}$$

$$\phi_{33} = n_c i_3 \frac{\mathcal{R}_1 + \mathcal{R}_2}{N} \tag{17}$$

To obtain the complete expression of the flux ϕ_1, the terms in the right-hand size of equation (1) were replaced to the ones presented in equations (6), (11) and (15). Doing the same for the other poles, the expressions of total flux in function of the reluctance and currents in the coils are given by equations (18) to (20).

$$\phi_1 = \frac{n_c}{N}[(\mathcal{R}_2 + \mathcal{R}_3)i_1 + \mathcal{R}_3 i_2 - \mathcal{R}_2 i_3] \tag{18}$$

$$\phi_2 = \frac{n_c}{N}[-\mathcal{R}_3 i_1 - (\mathcal{R}_1 + \mathcal{R}_3)i_2 - \mathcal{R}_1 i_3] \tag{19}$$

$$\phi_3 = \frac{n_c}{N}[-\mathcal{R}_2 i_1 + \mathcal{R}_1 i_2 + (\mathcal{R}_1 + \mathcal{R}_2)i_3] \tag{20}$$

As expected, the sum of all three fluxes is zero, due to the magnetic flux conservation in a closed path. With the help of the right-hand rule to find the flux direction when there are currents in all three coils, the result is shown in Figure 9.

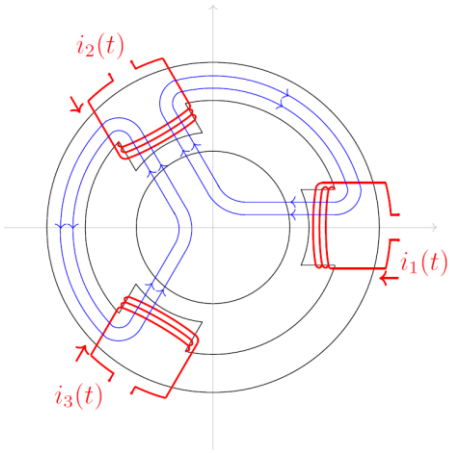

Figure 9. Flux direction resulted by the three currents in the coils.

The reluctance forces have the same direction of the magnetic flux and absolute values proportional to the square of each magnetic flux. As cited in [2], by Amperes-law and principle of virtual work, the formula for each force is given by equation (21). These forces are always attractive, as shown in Figure 10.

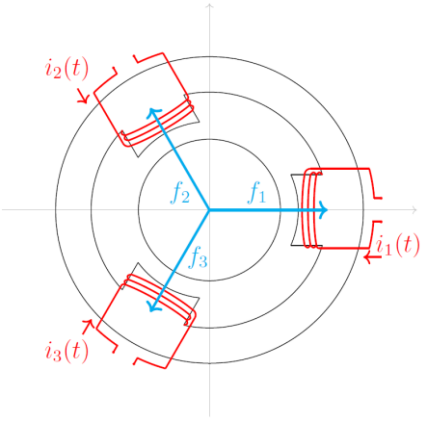

Figure 10. Reluctance forces associated with each pole.

$$f_k = \frac{\phi_k^2}{2\mu_0 A_c}, k = 1, 2, 3 \tag{21}$$

In steady-state the rotor operates at the equilibrium point and the resulting force is zero. Due to the three forces being separated by each other 120º, in steady-state operation it is necessary that all forces have the same module. For this

situation to occur, from equation (21), the magnetic fluxes must have the relation $(\phi_1)^2=(\phi_2)^2=(\phi_3)^2$.

In the three-pole magnetic bearing heteropolar configuration the magnetic flux of one pole will always be the sum of the other two, in this example, $(\phi_2)^2=(\phi_1+\phi_3)^2$ and therefore it is not possible for the equilibrium condition to be satisfied. Even if only two coils are used, the asymmetry of the configuration does not allow that the forces cancel each other. This rule out the use of the three-pole magnetic bearing in the upright position, in which the rotor needs to maintain equilibrium only by the reluctance forces.

However, with the magnetic bearing being placed in the horizontal position, the gravity force will act radially in the system and compose its resultant force, it is feasible to think about a certain orientation angle θ in which all forces can cancel each other. The Figure 11 shows the magnetic bearing in an arbitrary orientation and all three reluctance forces are decomposed in horizontal and vertical component, f_x and f_y respectively.

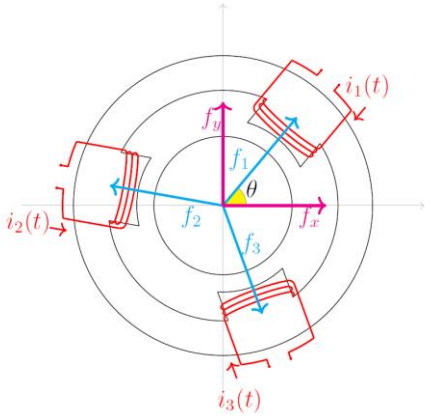

Figure 11. Magnetic Bearing in an arbitrary orientation angle, with the three reluctance forces decomposed in horizontal and vertical components.

The horizontal force f_x is the sum of each horizontal component of the force, and f_y is the sum of each vertical component, as shown by equations (22) and (24). Replacing each force using the equation (21), one can find the expressions in function of the corresponding magnetic fluxes, given by (23) and (25). The main objective with this operation is to find a relation between the input currents and the output reluctance resultant force.

$$f_x = f_1\cos(\theta) + f_2\cos\left(\theta+\frac{2\pi}{3}\right) + f_3\cos\left(\theta-\frac{2\pi}{3}\right) \tag{22}$$

$$f_x = \frac{1}{2\mu_0 A_c}\left[\phi_1^2\cos(\theta) + \phi_2^2\cos\left(\theta+\frac{2\pi}{3}\right) + \phi_3^2\cos\left(\theta-\frac{2\pi}{3}\right)\right] \tag{23}$$

$$f_y = f_1\sin(\theta) + f_2\sin\left(\theta+\frac{2\pi}{3}\right) + f_3\sin\left(\theta-\frac{2\pi}{3}\right) \tag{24}$$

$$f_y = \frac{1}{2\mu_0 A_c}\left[\phi_1^2\sin(\theta) + \phi_2^2\sin\left(\theta+\frac{2\pi}{3}\right) + \phi_3^2\sin\left(\theta-\frac{2\pi}{3}\right)\right] \tag{25}$$

When small displacements of the rotor occur, let's say of x units in horizontal and y in the vertical, the corresponding reluctances are given by equation (26) to (28).

$$\mathcal{R}_1 = \frac{1}{\mu_0 A_c}\left[h - x\cos(\theta) - y\sin(\theta)\right] \tag{26}$$

$$\mathcal{R}_2 = \frac{1}{\mu_0 A_c}\left[h + x\cos\left(\frac{\pi}{3}-\theta\right) - y\sin\left(\frac{\pi}{3}-\theta\right)\right] \tag{27}$$

$$\mathcal{R}_3 = \frac{1}{\mu_0 A_c}\left[h - x\cos\left(\frac{2\pi}{3}-\theta\right) + y\sin\left(\frac{2\pi}{3}-\theta\right)\right] \tag{28}$$

The coils currents can be separated in two terms, given by equation (29). One term is the base current (I_{0j}), responsible to provide the largest part of the magnetic flux that guarantees the equilibrium in steady state. The other term is the differential current (i_{dj}), that is important especially during transient or dynamic changes, these parcel help to adjust the reluctances forces necessary to centralize the rotor.

$$i_j = I_{0j} + i_{dj}, j = 1,2,3 \tag{29}$$

In [2] this problem was presented and is shown that the orientation angle that allow to reduce the number of amplifiers from three to two and still maintain the system's stability during transient is θ = π/6. The Figure 12 shows the magnetic bearing in the called "optimal orientation angle" with indication of the reluctance forces and the gravity force, and Figure 13 shows the path made by the magnetic flux.

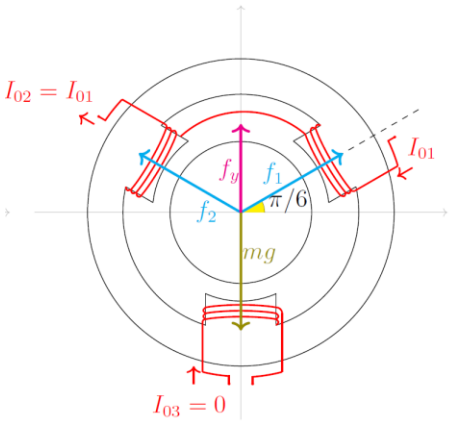

Figure 12. Force diagram for the magnetic bearing in the optimal orientation angle, that allows only one amplifier for coils 1 and 2. The situation pictured should occur in steady state operation.

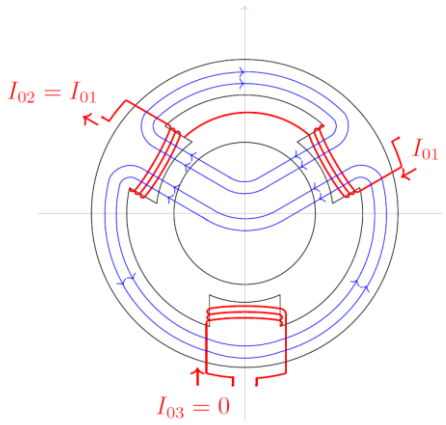

Figure 13. Magnetic flux path when the stator is oriented in the optimal orientation angle. The situation pictured should occur in steady state operation.

Using the information θ = π/6 in equations (26) to (28), the reluctances are given by equations (30) to (32).

$$\mathcal{R}_1 = \frac{1}{\mu_0 A_c}\left(h - \frac{\sqrt{3}}{2}x - \frac{1}{2}y\right) \tag{30}$$

$$\mathcal{R}_2 = \frac{1}{\mu_0 A_c}\left(h + \frac{\sqrt{3}}{2}x - \frac{1}{2}y\right) \tag{31}$$

$$\mathcal{R}_3 = \frac{h+y}{\mu_0 A_c} \tag{32}$$

Using this value of theta in equations (23) and (25), the horizontal and vertical forces are given by equations (33) and (34).

$$f_x = \frac{\sqrt{3}}{4\mu_0 A_c}(\phi_1^2 - \phi_2^2) \tag{33}$$

$$f_y = \frac{1}{4\mu_0 A_c}(\phi_1^2 + \phi_2^2 - 2\phi_3^2) \tag{34}$$

To find the complete expressions of f_x and f_y as function of the input currents, it is necessary to replace the reluctances found from (30) to (32) in equations (18) to (20), and finally replace them in (33) and (34). The results are very complicated multivariable nonlinear formulas, given by equations (35) and (36).

$$f_x = \frac{4}{3}\mu_0 A_c n_c^2 \; q_x(h, x, y, I_{01}, i_{d1}, i_{d3}) \tag{35}$$

$$f_y = \frac{2}{3}\mu_0 A_c n_c^2 \; q_y(h, x, y, I_{01}, i_{d1}, i_{d3}) \tag{36}$$

In which the terms q_x and q_y are shown in equation (37), the variable Δ is shown in equation (38) and the terms N_1 and N_2 in equations (39) and (40), respectively.

$$q_x(h, x, y, I_{01}, i_{d1}, i_{d3}) = \frac{N_1}{\Delta^2} \qquad q_y(h, x, y, I_{01}, i_{d1}, i_{d3}) = \frac{N_2}{\Delta^2} \tag{37}$$

$$\Delta = (x^2 + y^2 - 4h^2) \tag{38}$$

$$\begin{aligned} N_1 = {} & 6I_{01}^2 hx + 3I_{01}^2 xy - 4\sqrt{3}I_{01}h^2 i_{d3} + 12I_{01}hi_{d1}x + \\ & 6I_{01}i_{d1}xy - \sqrt{3}I_{01}i_{d3}x^2 + \sqrt{3}I_{01}i_{d3}y^2 - \\ & 4\sqrt{3}h^2 i_{d1}i_{d3} + 6hi_{d1}^2 x + 2hi_{d3}^2 x + 3i_{d1}^2 xy - \\ & \sqrt{3}i_{d1}i_{d3}x^2 + \sqrt{3}i_{d1}i_{d3}y^2 - i_{d3}^2 xy \end{aligned} \tag{39}$$

$$\begin{aligned} N_2 = {} & 12I_{01}^2 h^2 + 12I_{01}^2 hy - 3I_{01}^2 x^2 + 3I_{01}^2 y^2 + \\ & 24I_{01}h^2 i_{d1} + 24I_{01}hi_{d1}y - 6I_{01}i_{d1}x^2 + \\ & 6I_{01}i_{d1}y^2 - 4\sqrt{3}I_{01}i_{d3}xy + 12h^2 i_{d1}^2 - 4h^2 i_{d3}^2 + \\ & 12hi_{d1}^2 y + 4hi_{d3}^2 y - 3i_{d1}^2 x^2 + 3i_{d1}^2 y^2 - \\ & 4\sqrt{3}i_{d1}i_{d3}xy + i_{d3}^2 x^2 - i_{d3}^2 y^2 \end{aligned} \tag{40}$$

The region of analysis is near the equilibrium point $P_0 = (x, y, i_{d1}, i_{d3}) = (0, 0, 0, 0)$ so it is reasonable to linearize the equations (35) and (36) by Taylor expansion series and evaluate at the equilibrium point. The result of the linearization is shown in equations (41) and (42).

$$f_x = \frac{1}{2}k_p x - \frac{\sqrt{3}}{3}k_i i_{d3} \tag{41}$$

$$f_y = \frac{1}{2}k_p y + k_i i_{d1} \tag{42}$$

And the terms k_p and k_i are given by the expressions (43) and (44):

$$k_p = \frac{\mu_0 A_c n_c^2 I_{01}^2}{h^3} \tag{43}$$

$$k_i = \frac{\mu_0 A_c n_c^2 I_{01}}{h^2} \tag{44}$$

III. MECHANICAL DYNAMICS

As was showed in section before, the three-pole magnetic bearing can't be used in the upright position. So, to analyze the mechanical dynamics it is considered the systems as pictured in Figure 13, where the gravity has radial action in the system, the z-axis is axial to the rotor and the extremity of the shaft in the origin is supported by an axial bearing.

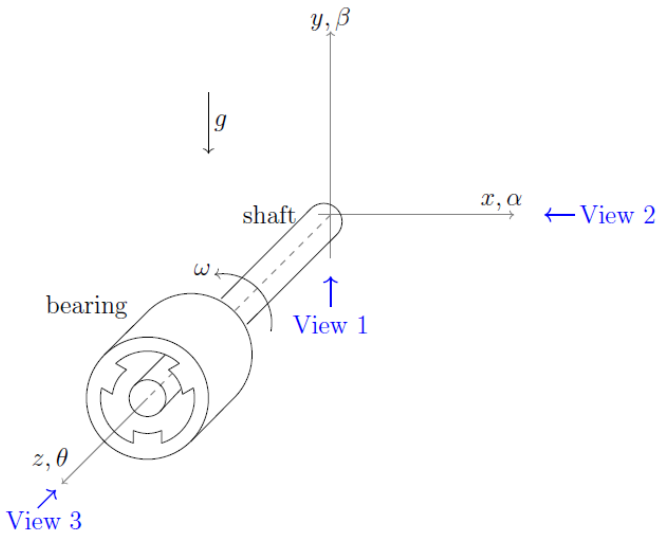

Figure 14. Three-Pole magnetic bearing geometry and orientation in a 3D axis.

In an ideal situation, the rotor center coincides with the z-axis. However, due to external factors, they don't coincide, and it is necessary to analyze its operation under perturbations and external factors. Figure 15 shows the situation, from view 3, where the axis is operating with displacements of x_b units in horizontal and y_b units in the vertical.

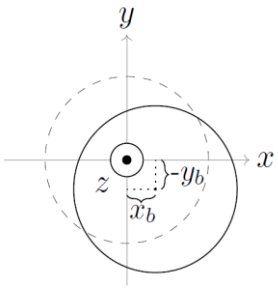

Figure 15. View 3. Horizontal and vertical displacements of the rotor.

Using the same formulation presented in [10] and [11] it is possible to analyze the spatial dynamics as two 2D coupled movements, one rotation around the *y*-axis and other rotation around the *x*-axis. Due to symmetry, the torque in *y* axis is equal to torque in *x* axis and will be named *J*.

Analyzing separately only the movement around the *y*-axis, as shown in Figure 16a, E_β is the angular moment related to this movement and the torque contribution from *x* axis is zero, so the rotational dynamic is presented in equation (45). Similarly, the rotation movement around the *x* axis is presented in Figure 16b, with E_α being the angular movement associated and the rotational dynamic given in equation (46).

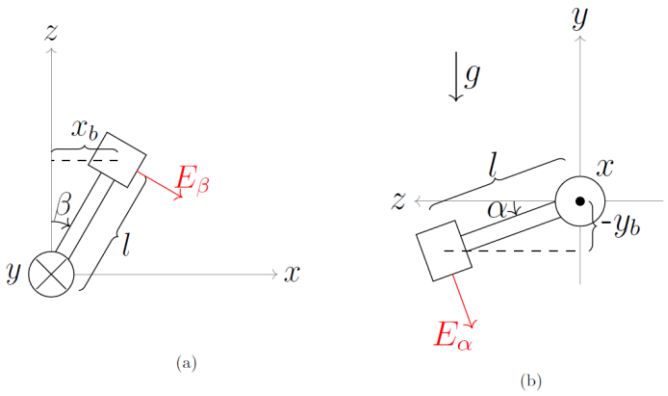

Figure 16. (a) View 1 (b) View 2.

$$J\ddot{\beta} - \omega I_z \dot{\alpha} = E_\beta \tag{45}$$

$$J\ddot{\alpha} + \omega I_z \dot{\beta} = E_\alpha \tag{46}$$

These two equations can be written in vector form, as equation (47).

$$J\ddot{\boldsymbol{p}} + G\dot{\boldsymbol{p}} = \mathbf{E} \tag{47}$$

Where ***p***, *G* and **E** are given by equation (48)

$$\boldsymbol{p} = \begin{bmatrix} \beta \\ -\alpha \end{bmatrix} \quad , \quad \mathbf{E} = \begin{bmatrix} E_\beta \\ -E_\alpha \end{bmatrix} \quad \text{e} \quad G = \begin{bmatrix} 0 & \omega I_z \\ -\omega I_z & 0 \end{bmatrix} \tag{48}$$

The vector **E** represents the torques caused by external factors. In this paper are considered the torques coming from the following excitations: Magnetic ($\mathbf{E}_m$), Gravitational ($\mathbf{E}_g$), Supporting Bearing ($\mathbf{E}_a$) and Mass Unbalance ($\mathbf{E}_d$). So, **E** can be expressed by equation (49).

$$\mathbf{E} = \mathbf{E}_\mathbf{m} + \mathbf{E}_\mathbf{g} + \mathbf{E}_\mathbf{a} + \mathbf{E}_\mathbf{d} \tag{49}$$

The Magnetic excitation come from the torque generated by the magnetic forces given in equations (41) and (42). Considering that α and β are small angles and *l* is the size of the shaft, the magnetic excitation is given by equation (50).

$$\mathbf{E}_\mathbf{m} = \frac{1}{2} l^2 k_p \boldsymbol{p} + l k_i \boldsymbol{u} \tag{50}$$

The term $\mathbf{E}_m$ and ***u*** are defined by (51), P_β and P_α are the torques associated to the *y*-axis and *x*-axis, respectively.

$$\mathbf{E}_\mathbf{m} = \begin{bmatrix} P_\beta \\ -P_\alpha \end{bmatrix} \quad e \quad \boldsymbol{u} = \begin{bmatrix} -\frac{\sqrt{3}}{3} i_{d3} \\ i_{d1} \end{bmatrix} \tag{51}$$

The rotor is positioned in a way that the gravity acts radially, so the weight produces torque only around the *x*-axis, as shown in Figure 17. Considering the center of mass of the system located *h* units from the origin (ideally, *h* = *l*), the torque would be given by $mg\ cos(\alpha)h \approx mgh$. So, the Gravitational excitation is given by equation (52).

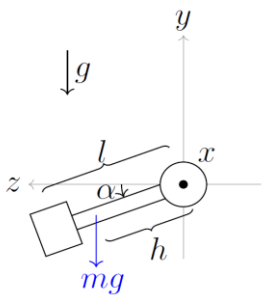

Figure 17. (b) View 2, showing the action of gravity force in the system.

$$\mathbf{E}_{\mathrm{g}} = \begin{bmatrix} 0 \\ mgh \end{bmatrix} = mgh \underbrace{\begin{bmatrix} 0 \\ 1 \end{bmatrix}}_{e_2} = mgh\boldsymbol{e_2} \tag{52}$$

The axial bearing has viscous damping, with the torques being proportional to the displacements' angular velocities in each axis. The supporting bearing excitation ($\mathbf{E}_{\mathrm{a}}$) is given by equation (53), given that C_{a} is a constant.

$$\mathbf{E}_{\mathbf{a}} = -C_a \begin{bmatrix} \dot{\beta} \\ -\dot{\alpha} \end{bmatrix} = -C_a \dot{\boldsymbol{p}} \tag{53}$$

Identically as described in [10], where variable m corresponds to the value of a small mass placed in the rotor causing unbalance, q is a factor, $0 < q < 1$, that measures how distant the mass is from the radius r of the rotor and the angular speed is ω. The mass unbalance excitation ($\mathbf{E}_{\mathrm{d}}$) is given by equation (54).

$$\mathbf{E}_{\mathrm{d}} = \underbrace{mrq\omega^2}_{\Delta} \underbrace{\begin{bmatrix} \cos(\omega t) \\ -\sin(\omega t) \end{bmatrix}}_{\boldsymbol{v}(\omega,t)} = \Delta\boldsymbol{v}(\omega,t) \tag{54}$$

Replacing the equations (50) to (54) in (49), and then in (47), the rotational dynamic can be written in equation (55).

$$J\ddot{\boldsymbol{p}} + (G + C_a I_2)\dot{\boldsymbol{p}} - \frac{1}{2} l^2 k_p \boldsymbol{p} = lk_i \boldsymbol{u} + \underbrace{mgh\boldsymbol{e_2}}_{\mathbf{E_g}} + \Delta\boldsymbol{v}(\omega,t) \tag{55}$$

Defining the vector $\boldsymbol{p_s}$ with the components x_s and y_s measured by the sensors, in which $x_s = \beta d$ and $y_s = -\alpha d$, $d \neq 0$, with d being the distance from the origin to the sensor. The relation between $\boldsymbol{p_s}$ and $\boldsymbol{p}$ is given by equation (56).

$$\boldsymbol{p_s} = \begin{bmatrix} x_s \\ y_s \end{bmatrix} = d \begin{bmatrix} \beta \\ -\alpha \end{bmatrix} = d\boldsymbol{p} \tag{56}$$

With some algebraic manipulations, it is possible to rewrite equation (55) in terms of $\boldsymbol{p_s}$, shown in equation (57).

$$\ddot{\boldsymbol{p}}_{\boldsymbol{s}} + G_e \dot{\boldsymbol{p}}_{\boldsymbol{s}} - K_e \boldsymbol{p_s} = k_j l k_i \boldsymbol{u} + k_j(\mathbf{E}_{\mathrm{g}} + \Delta\boldsymbol{v}(\omega,t)) \tag{57}$$

Where the terms G_e, K_e and k_j are explicit in equations (58), (59) and (60).

$$G_e(\omega) = J^{-1}(G + C_a I_2) = J^{-1} \begin{bmatrix} C_a & \omega I_z \\ -\omega I_z & C_a \end{bmatrix} \tag{58}$$

$$K_e = \frac{1}{2} J^{-1} l^2 k_p \tag{59}$$

$$k_j = J^{-1} d \tag{60}$$

Furthermore, considering the state vector $\boldsymbol{x}$ as pointed in equation (61), with its states being the positions measured by the sensors and its derivatives.

$$\boldsymbol{x} = \begin{bmatrix} \boldsymbol{p_s} & \dot{\boldsymbol{p}}_{\boldsymbol{s}} \end{bmatrix}^T = \begin{bmatrix} x_s & y_s & \dot{x}_s & \dot{y}_s \end{bmatrix}^T \tag{61}$$

Deriving equation (61) and using the information from equation (57) gives the dynamical equation:

$$\dot{\boldsymbol{x}}(t) = A(\omega)\boldsymbol{x}(t) + B\boldsymbol{u}(t) + \boldsymbol{k}(\omega,t) \tag{62}$$

In which the terms $A(\omega)$, B, $\boldsymbol{k}(\omega,t)$ is given by:

$$A(\omega) = \begin{bmatrix} 0_2 & I_2 \\ K_e I_2 & -G_e(\omega) \end{bmatrix}, \quad B = \begin{bmatrix} 0_2 \\ k_j l k_i I_2 \end{bmatrix} \tag{63}$$

$$\boldsymbol{k}(\omega,t) = \begin{bmatrix} 0_2 \\ k_j I_2 \end{bmatrix} (\mathbf{E}_{\mathrm{g}} + \Delta\boldsymbol{v}(\omega,t)) \tag{64}$$

And I_2 is the 2x2 identity matrix and 0_2 is the 2x2 zero matrix. Fixing the analysis in one constant angular speed (ω), the matrix $A(\omega)$ become constant, A, and $\boldsymbol{k}(\omega,t)$ (a disturbance in the system) become only dependent of time, $\boldsymbol{k}(t)$. So, equation (62) can be rewritten as:

$$\dot{\boldsymbol{x}}(t) = A\boldsymbol{x}(t) + B\boldsymbol{u}(t) + \boldsymbol{k}(t) \tag{65}$$

For small displacements of the rotor, the output of this control system are the reluctance forces given by equation (41) and (42), here written in vector form:

$$\boldsymbol{f} = \begin{bmatrix} fx \\ fy \end{bmatrix} \tag{66}$$

The x and y variables from equations (41) and (42) can be replaced by x_s and y_s, so $\boldsymbol{f}$ is given by:

$$\boldsymbol{f} = \frac{1}{2} k_p l I_2 \begin{bmatrix} \beta \\ -\alpha \end{bmatrix} + k_i \begin{bmatrix} -\frac{\sqrt{3}}{3} i_{d3} \\ i_{d1} \end{bmatrix} \tag{67}$$

And after few manipulations results in the expression:

$$\boldsymbol{f} = C\boldsymbol{x} + D\boldsymbol{u} \tag{68}$$

Where C and D are given by:

$$C = \frac{1}{2} \frac{k_p l}{d} \begin{bmatrix} I_2 & 0_2 \end{bmatrix}, \quad D = k_i \tag{69}$$

The block diagram of the linearized system, corresponding to the state-space equations (65) and (68), is shown in Figure 18. Due to linearization, this block diagram is valid only near the equilibrium point, i.e., for smalls values of axis displacement.

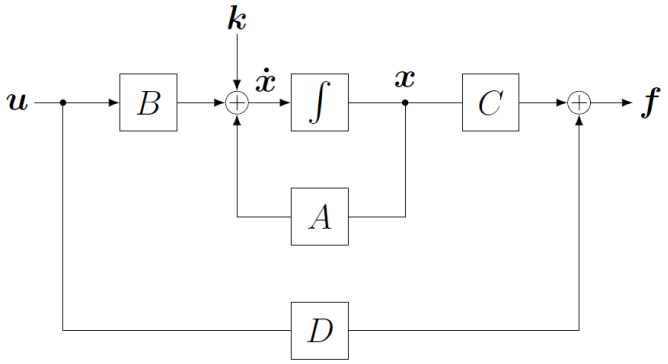

Figure 18. Block Diagram of the Linear Dynamical System from the Three-Pole Magnetic Bearing Model.

Linear Control techniques can be used to find the input currents $\boldsymbol{u}$ that best meet the control needs, especially regarding the stability of the rotor, preferably with the minimum power consumption.

IV. COMMENTS AND CONCLUSION

A detailed look at the linearized model for the three-pole heteropolar magnetic bearing was presented. Although the reluctances forces have strong nonlinear behavior, near the equilibrium point the linearization is a valid technique to analyze the relation between the input control currents and the output forces.

Furthermore, real systems are subjected to external disturbances that may influence its dynamical behavior. This study also presents a state-space representation of the system considering four types of external disturbances, under the conditions that the rotor has constant angular speed and small displacements over its axial direction. The control problem for this system will be studied in a future work.

REFERENCES

[1] W. Zhang and H. Zhu, "Radial magnetic bearings: An overview", Results in Physics, vol. 7, pp. 3756-3766, 2017.

[2] S.L. Chen and C.T. Hsu, "Optimal design of a three-pole active magnetic bearing", IEEE Transactions on Magnetics, vol 38, no. 5,2, pp. 3458-3466, 2002.

[3] C.T. Hsu and S.L. Chen, "Exact linearization of a voltage-controlled 3-pole active magnetic bearing system", IEEE Transactions on Control Systems Technology, vol. 10, no. 4, pp. 618-625, 2002.

[4] C.T. Hsu and S.L. Chen, "Nonlinear control of a 3-pole active magnetic bearing system", Automatica, vol. 39, no. 2, pp. 291-298, 2003.

[5] S.L. Chen, S.H. Chen and S.T. Yan, "Experimental validation of a current-controlled three-pole magnetic rotor-bearing system", IEEE Transactions on Magnetics, vol. 41, no. 1,1, pp. 99-112, 2005.

[6] D.C. Meeker and E.H. Maslen, "Analysis and Control of a Three Pole Radial Magnetic Bearing", Tenth International Symposium on Magnetic Bearings, 2006.

[7] S.L. Chen and C.C. Weng, "Robust Control of a Voltage-Controlled Three-Pole Active Magnetic Bearing System", IEEE-ASME Transactions on Mechatronics, vol. 15, no. 3, pp. 381-388, 2010.

[8] M. Kiani, H. Salarieh, A. Alasty and S.M. Darbandi, "Hybrid control of a three-pole active magnetic bearing", Mechatronics, vol. 39, pp. 28-41, 2016.

[9] S.L. Chen and K.Y. Liu, "Sensorless Control for a Three-pole Active Magnetic Bearing System", Applied Computational Electromagnetics Society Journal, vol. 32, no. 8, pp. 720-725, 2017.

[10] D.F.B. David, J.A. Santisteban and A.C.D.N. Gomes, "Modeling and Testing Strategies for an Interconnected Four-Pole Magnetic Bearing", Actuators, vol. 6, no. 3, 2017.

[11] A. Chiba, T. Fukao, O. Ichikawa, M. Oshima, M. Takemoto and D. G. Dorell, "Magnetic Bearings and Bearingless Drives", Elsevier, 2005.